

Astronomy & Astrophysics manuscript no.
(will be inserted by hand later)

Apparent radii of neutron stars, observations of Geminga and RX J185635-3754, and equation of state of dense matter

P. Haensel

N. Copernicus Astronomical Center, Polish Academy of Sciences, Bartycka 18, PL-00-716 Warszawa, Poland
e-mail: haensel@camk.edu.pl

Received 15 May, 2001/Accepted xx xxxx

Abstract. Apparent (radiation) radius of neutron star, R_∞ , depends on the star gravitational mass in quite a different way than the standard coordinate radius in the Schwarzschild metric, R . We show that, for a broad set of equations of state of dense matter, the lower bound on R_∞ at fixed M , $R_{\infty,\min}(M)$, resulting from the very definition of R_∞ , is very close to $R_\infty(M_{\max})$ for the configurations with maximum allowable masses. Also, this absolute lower bound is only 0.6% lower than the value corresponding to the maximum compactness of neutron star consistent with general relativity and condition $v_{\text{sound}} < c$. Estimates of R_∞ for Geminga and RX J185635-3754 are consistent, within 2σ , with all considered equations of state, provided the detected photon spectra are fitted using the atmosphere models, and neutron star mass is above $0.2M_\odot$. If one fitted the RX J185635-3754 photon spectrum with black body one, the resulting upper bound on R_∞ would imply that this compact object is a low-mass strange star covered with a normal matter envelope; such a possibility, however, seems to be excluded by the optical part of the detected spectrum.

Key words. dense matter – equation of state – stars: neutron – stars

1. Introduction

Observations of isolated neutron stars give a unique opportunity of studying neutron star properties without complications resulting from the magnetosphere (radio pulsars) or accretion flows (X-ray pulsars and bursters, low-mass X-ray binaries). Measuring the spectrum of radiation from neutron star surface (or, more precisely, atmospheres), combined with knowledge of distance (from measuring of the annual parallax) enables one, in principle, to determine total luminosity, effective surface temperature, and neutron star radius. Recently, such studies have been carried out for Geminga (Golden & Shearer 1999) and RX J185635-3754 (Walter 2001).

Neutron star are relativistic objects, and for masses above solar mass their radii may be only 1.5 - 2 times larger than the gravitational (Schwarzschild) radius $r_g \equiv 2GM/c^2 = 2.95 (M/M_\odot)$ km. Therefore, because of a sizable spacetime curvature close to neutron star, one has to distinguish between the “true” or “coordinate” radius, R , which is the radial coordinate of the stellar surface in the Schwarzschild metric, and the “apparent radius” (sometimes called “radiation radius”), R_∞ , as determined by a distant observer studying radiation from neutron star surface.

In the present letter we calculate dependence of R_∞ on neutron star mass for a broad set of equations of state of dense matter. Then, we determine lower bounds on $R_\infty(M)$, and finally we confront theoretical calculations with recent measurements of R_∞ for Geminga and RX J185635-3754.

2. $R(M)$, $R_\infty(M)$, and their theoretical lower bounds

The effective surface temperature, T_s , at the neutron star surface, is related to total photon luminosity, L_γ , by

$$L_\gamma = 4\pi R^2 \sigma_{\text{SB}} T_s^4 , \quad (1)$$

where all quantities are measured by a local observer on neutron star surface. Spherical symmetry is assumed. A distant observer (“at infinity”) will measure “apparent luminosity” L_γ^∞ , “apparent effective temperature” T_s^∞ , and “apparent radius” R_∞ , related to quantities appearing in Eq.(1) by (Thorne 1977)

$$L_\gamma^\infty = L_\gamma \left(1 - \frac{r_g}{R}\right) = 4\pi R_\infty^2 \sigma_{\text{SB}} (T_s^\infty)^4 ,$$

$$T_s^\infty = T_s \sqrt{1 - \frac{r_g}{R}} , \quad R_\infty = \frac{R}{\sqrt{1 - r_g/R}} . \quad (2)$$

As we will show, dependence of R_∞ on neutron star mass differs considerably from $R(M)$; the difference, which re-

Table 1. Distance and apparent radii calculated for two close by isolated neutron stars. The values obtained by fitting the black body spectrum is denoted by “BB”. Atmospheric models of the spectra lead to values labeled by “atm”. Error bars correspond to 1σ (67%) confidence level. The upper bounds on measured R_∞ are given at the 2σ (95%) confidence level.

neutron star (reference)	d (pc)	R_∞		upper bound on R_∞	
		BB (km)	atm (km)	BB (km)	atm (km)
RX J185635-3754 (Walter 2001)	61^{+9}_{-8}	$6.0^{+1.2}_{-0.6}$	$11.2^{+3.4}_{-3.4}$	8.4	18.0
Geminga (Golden & Shearer 1999)	159^{+59}_{-34}	$\leq 9.5^{+3.5}_{-2.0}$	$\leq 10.0^{+3.8}_{-2.1}$	16.5	17.6

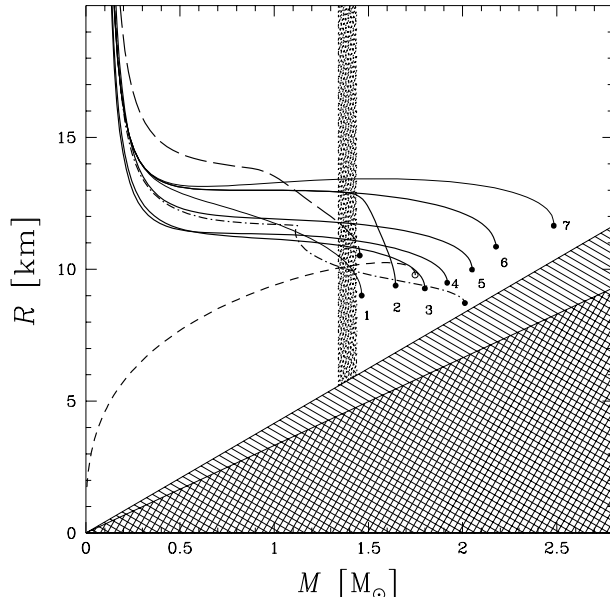


Fig. 1. Neutron star radius R versus gravitational mass M , for seven EOS of baryonic matter, labeled by numbers 1-7. 1: BPAL12 of Bombaci et al. (1995); 2: EoS1H1 of Balberg et al. (1999); 3: FPS of Pandharipande & Ravenhall (1989); 4: Baldo et al. (1997); 5: Douchin & Haensel (2000); 6: EoS1 of Balberg et al. (1999); 7: EoS2 of Balberg et al. (1999). Dotted line corresponds to strange stars built of self-bound quark matter (SQ1, Haensel et al. 1986). Long dashes: hybrid neutron stars of dense matter with a mixed baryon-quark phase, EOS from Table 9.1 of Glendenning (1997). Long dashes-dot line: EOS with first-order phase transition to a pure kaon-condensed matter (Kubis 2001). Doubly hatched area is prohibited by general relativity and corresponds to $R < \frac{9}{8}r_g$. Singly hatched area is excluded by general relativity combined with condition $v_{\text{sound}} < c$. In the case of stars built of baryonic matter, configurations with maximum allowable mass is indicated by a filled circle, and in the case of strange stars, built of self-bound quark matter - by an open circle. Shaded vertical band corresponds to the range of precisely measured masses of binary radio pulsars.

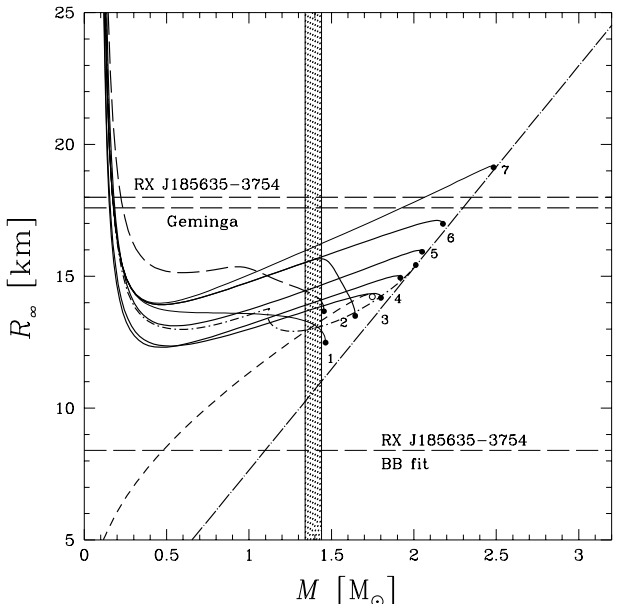


Fig. 2. Apparent radius of neutron star, R_∞ , versus gravitational mass, M . Notation as in Fig. 1. Thick long-dash-dot straight line corresponds to minimum R_∞ at a given M . Thick dashed horizontal lines correspond to 2σ lower bounds on R_∞ of two close by isolated neutron stars, obtaining using model atmosphere spectra. Much lower thin dashed line was obtained using a black body fit to the detected photon spectrum.

fects spacetime curvature near neutron star, increases with increasing M , and becomes quite large at the maximum allowable mass, M_{max} . The curves $R(M)$ and $R_\infty(M)$, calculated for a broad set of equations of state (EOS) of dense matter, are presented in Fig. 1 and Fig. 2, respectively. One notices, that for moderately stiff and stiff equations of state ($M_{\text{max}} > 1.8 M_\odot$) without a strong softening at highest densities, for $M > 0.5 M_\odot$ the apparent radius R_∞ increases with increasing M (except for a tiny region close to M_{max}), in contrast to $R(M)$, which decreases in the same mass interval.

In Fig. 1, straight lines, marking upper boundaries of the hatched regions of the $R - M$ plane, result from

quite general physical conditions imposed on the configurations of hydrostatic equilibrium in general relativity. The lower boundary results from the condition that pressure within an equilibrium configuration should be finite, and can be expressed as $R(M) > \frac{9}{8}r_g$ (general proof can be found in Weinberg 1972). This condition can be rewritten as $R(M) > R_{\min 1}(M) = 3.32 (M/M_\odot)$ km. A stronger condition is obtained if we additionally require that sound speed within the star should be subluminal: $v_{\text{sound}} = \sqrt{dP/d\rho} < c$ (such a condition is *necessary*, but *not sufficient* (Olson 2000), to respect causality in a fluid medium). This leads to $r_g/R < 0.7081$ (calculations of Lindblom (1983) implied 0.72, we use more precise determination of this limit by Haensel et al. 1999), which implies $R(M) > R_{\min 2}(M) = 4.17 (M/M_\odot)$ km.

A strict lower bound on $R_\infty(M)$ results from the very definition of R_∞ . This definition implies

$$\frac{R_\infty}{r_g} = \frac{R}{r_g \sqrt{1 - r_g/R}}. \quad (3)$$

The right-hand-side of the above equation is a function of $x \equiv r_g/R$ only. It diverges to $+\infty$ at $x = 0$ and at $x = 1$. At fixed M , it has a single minimum at $x = 2/3$. Therefore, minimum value of $R_\infty(M)$ is $R_{\infty,\min}(M) = 7.66 (M/M_\odot)$ km (see also Lattimer & Prakash 2001).

Let us notice, that this limiting R_∞ for an “apparently most compact” neutron star is very close to (but a little smaller than) that for a maximum compactness $x = 0.7081$ consistent with $v_{\text{sound}} < c$, given by $7.71 (M/M_\odot)$ km. However, at any M the difference is only 0.6%, and therefore in practice smallest R at a fixed M , consistent with $v_{\text{sound}} < c$, can be considered as corresponding to smallest $R_\infty(M)$, and vice versa.

This result can be easily understood, because $x = 0.7081$ is only by 0.05 higher than $2/3$ corresponding to the minimum of R_∞ . Therefore, relative difference between $R_{\infty,\min}$ and the value corresponding to minimum value of R at given M (assuming $v_{\text{sound}} < c$), can be estimated as $\simeq 2.25 \times (0.05)^2 = 0.6\%$, which is consistent with our exact result.

While the subluminal ($v_{\text{sound}} < c$) upper bound on x at given M is slightly larger than $2/3$, the *actual* maximum values of x for various EOS, which are reached at M_{\max} for these EOS, are lower than $2/3$. However, if we restrict to medium stiff and stiff EOS, with $M_{\max} \gtrsim 1.8 M_\odot$, then $x_{M_{\max}} \simeq 0.6$, which is only 0.06 lower than $2/3$. We may therefore expect, that for these EOS, which actually constitute majority of models in Figs. 1, 2, $(R_\infty)_{M_{\max}}$ will be only $\sim 2.25 \times (0.06)^2 \simeq 0.8\%$ larger than $R_{\infty,\min}$. This explains, why for these EOS the points at M_{\max} are so close to the $R_{\infty,\min}(M)$ line in Fig. 2.

A practical theoretical lower limit on R_∞ can also be deduced from Fig. 2. For any baryonic EOS, $R_\infty > 11$ km, independently of neutron star mass. On the contrary, there is no lower limit on R_∞ for bare strange stars, whose size can be as small as hundred fermis. For strange stars covered with a layer of normal matter, minimum radius is

reached at $M \sim 0.01 M_\odot$, and for a maximally thick crust it is about 5–6 km (see, e.g., Glendenning 1997).

3. Observational bounds on R_∞

In order to establish observational upper bounds on R_∞ of Geminga and RX J185635-3754, which could be then meaningfully confronted with theoretical predictions, one has first to analyze uncertainties in measured values of R_∞ for these isolated neutron stars.

3.1. Geminga

An important assumption in Golden & Shearer (1999) is that error in fitting the measured spectrum of radiation by a two-component model can be neglected, compared with the error in the distance d . Under this assumption, they determine two parameters: surface temperature T_s^∞ , and the ratio R_∞/d . Neglecting the error in T_s^∞ , the uncertainty in R_∞ results thus from the uncertainty in d . The distance to Geminga has been determined from the measurement of the annual parallax by Caraveo et al. (1996). These authors used the optical data from the *Hubble Space Telescope (HST)* observations, and obtained $d = 159^{+59}_{-34}$ pc. Notice, that if the error in fitting the radiation spectrum is neglected, the upper bound on the apparent radius corresponds to the lower bound on d . In our opinion, in order to be meaningful, the upper bound on R_∞ should be determined at the 2σ (i.e., 95%) confidence level. In such a case, we get $R_\infty < 17.6$ km assuming the H atmosphere, and $R_\infty < 16.5$ km for the black body thermal spectrum (which turns out to be practically indistinguishable from the Fe/Si model atmosphere spectrum). The value of the upper bound on the apparent radius of Geminga is therefore not very sensitive to the atmospheric model.

3.2. RX J185635-3754

As in the case of Geminga, what one actually determines (assuming a model for the photon spectrum) is T_s^∞ and R_∞/d . A relatively precise determination of the distance was possible, using *HST* observations over a three years period (Walter 2001). After disentangling annual parallax and the neutron star proper motion, Walter (2001) gets $d = 61 \pm 13$ pc at the 2σ (95%) confidence level. In order to determine T_s^∞ , one has to analyze the detected photon spectrum. An important additional piece of information on radiation spectrum comes from the optical *HST* observations (Walter & Matthews 1997). In this way, the X-ray (Walter et al. 1996) and extreme UV (Lampton et al. 1997) segments of the radiation spectrum are augmented by two points in the optical domain. The combined X-ray and optical data are much better fitted by the model atmosphere than by the black body spectrum (Walter & An 1998, Walter et al. 2000). This yields $R_\infty(\text{atm})/d = 0.18 \pm 0.05$ km/pc. Together with parallax determination of d , this implies $R_\infty(\text{atm}) = 11.2 \pm 6.8$ km at the 2σ confidence level. If one uses the black body

spectrum model (which seems to be inconsistent with optical data points), the corresponding value of T_s^∞ is significantly higher, and implies an abnormally small value $R_\infty(\text{BB}) = 6.0_{-1.2}^{+2.4}$ km (Walter 2001).

All in all, the upper bound on the apparent radius of RX J185635-3754 can be set at 18.0 km. The above bound is established at the 2σ (95%) confidence level, neglecting uncertainties connected with atmosphere spectrum.

3.3. Theory versus observations

The upper bounds (at 2σ confidence level) on the apparent radii of Geminga and RX J185635-3754 are compared with theoretical predictions for $R_\infty(M)$ in Fig.2. Neutron star models based on considered baryonic EOS of dense matter are consistent with these upper bounds, provided the mass of both compact sources is above $0.2 M_\odot$. If the EOS is as stiff as EOS 7, observational upper bounds on the apparent radii limit the mass of Geminga and RX J185635-3754 to $0.2 < M/M_\odot < 2$, not a very useful constraint.

Had we accepted the estimate $R_\infty(\text{BB})$ for RX J185635-3754, this object could be but a low-mass strange star. In order to produce thermal photon spectrum, this low-mass strange star should have been covered with a layer of normal matter, because a bare quark surface would be a too weak photon emitter (Chmaj et al. 1991, Usov 2001). However, the observed points in the optical part of the photon spectrum seem to exclude the black body model and to make such an exotic solution unnecessary.

4. Summary

Detection of photons emitted from the surface of isolated neutron stars of known distance can result in determination of the apparent neutron star radius, R_∞ . Due to significant space-time curvature, dependence of R_∞ on stellar mass is quite different from that of the standard "coordinate" radius R . The very definition of R_∞ implies a lower bound $7.66(M/M_\odot)$ km, and does not involve any constraint on the EOS of dense matter. At any M , this lower limit is very close to the value of R_∞ corresponding to the minimum R , calculated under the condition of subluminal sound. Simultaneously, the actual values of R_∞ calculated at the maximum allowable mass are also close to this limit. For moderately stiff and stiff EOS with $M_{\max} \gtrsim 1.8 M_\odot$, the actual value of $R_\infty(M_{\max})$ is less than one percent higher than the absolute lower bound on R_∞ at this value of stellar mass. Upper bounds on R_∞ of Geminga and RX J185635-3754, at the 2σ (95%) confidence level, are 17.6 km and 18.0 km, respectively. They are consistent with all considered EOS of baryonic matter, provided gravitational mass of these two isolated neutron stars is above $0.2 M_\odot$.

The fact that the model atmosphere fit to detected photon spectrum of RX J185635-3754 is strongly favored with respect to the black body one (Lattimer & Prakash

2001), is of crucial importance. For $R_\infty < 8.4$ km, obtained using the black body fit, neutron star models based on existing EOS are excluded, and a low-mass strange star covered with a layer of normal matter is a unique solution.

Determination of R_∞ for Geminga and RX J185635-3754 should be considered as a very preliminary attempt to measure radii of solitary, close by neutron stars, from the studies of their photon spectra. For the time being, the uncertainties in measured R_∞ are large. Additionally, due to very limited knowledge of the photon spectra, extracted values of the apparent radii depend on the assumed model of the neutron star atmosphere. One may hope, that future observations will enable determination of the atmosphere composition, via more detailed analysis of the photon spectra, and therefore will hopefully open the way to better measurement of the parameters of closeby, isolated neutron stars.

Acknowledgements. I am grateful to J.L. Zdunik for the reading of the manuscript and for helpful remarks. I am also grateful to A. Potekhin for his precious help in the preparation of figures. This research was partially supported by the KBN grant No. 5P03D.020.20.

References

- Balberg S., Lichtenstadt I., Cook G.B., 1999, ApJS 121, 515
- Baldo M., Bombaci I., Burgio G.F., 1997, A&A 328, 279
- Bombaci I., 1995, in: Perspectives on Theoretical Nuclear Physics, I. Bombaci, A. Bonaccorso, A. Fabrocini, A. Kievsky, S. Rosati, and M. Viviani, eds., p. 223
- Bondi H., 1964, Proc. Roy. Soc. A 281, 39
- Caraveo P.A., Bignami G.F., Mignani R., Taff L.G., 1996, ApJ 461, L91
- Chmaj T., Haensel P., Słomiński, 1991, Nucl.Phys.B 24B, 40
- Douchin F., P. Haensel P., 2000, Phys. Lett. B 485, 107
- Glendenning N.K., 1997, Compact Stars: Nuclear Physics, Particle Physics and General Relativity. Springer, New York
- Golden A., Shearer A., 1999, A&A 342, L5
- Haensel P., Zdunik J.L., Schaeffer R., 1986, A&A 160, 121
- Haensel P., Lasota J.P., Zdunik J.L., 1999, A&A 344, 151
- Kubis S., 2001, PhD Thesis, Jagellonian University (unpublished)
- Lampton M., Lieu R., Schmitt J.H.M.M., Bowyer S., Voges W., Lewis J., Wu X., 1997, ApJS 108, 545
- Lattimer J.M., Prakash M., 2001, ApJ 550, 426
- Lindblom L., 1984, ApJ 278, 364
- Olson T.S., 2001, Phys. Rev. C 63, 015802
- Pandharipande V.R., Ravenhall D.G., Proc. NATO Advanced Research Workshop on nuclear matter and heavy ion collisions, Les Houches, 1989, eds. M. Soyeur et al. (Plenum, New York, 1989) p.103
- Thorne K.S., 1977, ApJ 212, 825
- Usov V.V., 2001, ApJ 550, L179
- Walter F.M., Wolk S.J., Neuhäuser R., 1996, Nature 379, 233
- Walter F.M., Matthews L.D., 1997, Nature 389, 358
- Walter F.M., An P., 1998, BAAS 192, 50.04
- Walter F.M., An P., Lattimer J., Prakash M., 2000, in: IAU Symp. 195, Highly Energetic Physical Processes and Mechanisms for Emission from Astrophysical Plasmas, ed. P.C.H. Martens, S. Tsuruta, & M.A. Weber (ASP Conf. Ser., San Francisco, ASP), p.437

Walter F.M., 2001, ApJ 549, 433
Weinberg S., 1972, Gravitation and Cosmology: Principles and
Applications of the General Theory of Relativity, (John
Wiley & Sons, New York), Sect.11.6